IL NUOVO CIMENTO **47 C** (2024) 54
DOI 10.1393/ncc/i2024-24054-7

Colloquia: COMEX7

Indirect methods: A bridge between nuclei and stars

M. La Cognata(*)
INFN, Laboratori Nazionali del Sud - Catania, Italy

received 31 October 2023

Summary. — Nuclear reactions in stars generally take place at energies well below 1 MeV, therefore the Coulomb barrier exponentially suppresses the cross section down to values as small as few nanobarns in the case of charged particles. This makes it very difficult to provide accurate input data for astrophysics so indirect methods have been introduced. In particular, the ANC and the THM techniques have been used to deduce the cross sections of reactions with photons and charged particles in the exit channel, respectively, with no need of extrapolation. Recent results of the application of the two methods are discussed: the ^{6}Li(^{3}He,d)^{7}Be measurement used to deduced the ANC's of the $^{3}\mathrm{He} + {}^{4}\mathrm{He} \rightarrow {}^{7}\mathrm{Be}$ and $p + {}^{6}\mathrm{Li} \rightarrow {}^{7}\mathrm{Be}$ channels and the corresponding radiative-capture cross sections. The THM measurement of the $^{27}\mathrm{Al}(p,\alpha)^{24}\mathrm{Mg}$ cross section through the ^{2}H(^{27}Al,α ^{24}Mg)n reaction is also illustrated. In both cases, we were able to establish the cross section at astrophysical energies with unprecedented accuracy.

1. – Indirect methods

Indirect methods are those techniques making it possible to deduce the astrophysical factor [1] of a reaction by performing the measurement of the cross section of a related process, and by employing nuclear reaction theory to link the two. Such tools are especially necessary when nuclear reactions of astrophysical importance are investigated. Indeed, in astrophysics and especially in quiescent stellar evolutionary stages, energies of interest are so low that for charged particles the Coulomb barrier strongly lessens cross sections making their measurement essentially impossible. These energies (the so-called Gamow window [1]) usually vary between few keV and few hundreds of keV, so cross sections can be much smaller than 1 nb, making extrapolation from high energies mandatory. While the use of the astrophysical factor, a smoothly varying function of energy, helps reducing the systematic errors introduced by the extrapolation procedure, in the case of resonant reactions significant deviations from the smooth behaviour might be expected, due to unknown or unpredicted resonances. Even in the case of non-resonant cross sections, electron screening makes extrapolation very uncertain (see, for instance, [2] for

(*) E-mail: lacognata@lns.infn.it

a case study). Electron screening arises when interaction energies are comparable with the electron binding energies in atoms, so the presence of atomic electrons cannot be neglected. Electron clouds lead to an enhancement of the astrophysical factor related to the shielding of the nuclear charges by the surrounding negatively-charged electron clouds. Therefore, the bare-nucleus cross section, that is the parameter of interest for astrophysical applications, cannot be directly assessed with traditional beam and solid or gaseous target reactions and indirect methods are very helpful.

In the present work, we will focus on two indirect techniques. First, we will discuss the Trojan Horse Method (THM) [3]. The THM has been successfully used to investigate low-energy nuclear reactions induced by charged particles (see, *e.g.*, [4, 5]), including radioactive ion beams (*e.g.*, [7]), and neutrons (*e.g.*, [6]), with the exclusion of radiative capture processes. In particular, we will focus on the theoretical formalism named modified R-matrix, allowing for the analysis of multi-resonance reactions (see, *e.g.*, [8]). Radiative capture reactions are indirectly studied, among other approaches, by the extraction of the Asymptotic Normalization coefficient (ANC), especially suited for pure external direct capture processes [9].

2. – The THM applied to the ^{27}Al$(p,\alpha)^{24}$Mg reaction

In the THM general framework, the cross section of the $A(x,b)B$ reaction is obtained through the $A(a,bB)s$ reaction performed at energies much higher than the astrophysical ones (several tens of MeV), so that no Coulomb and centrifugal barriers in the entrance channel hinder the cross section, neither electron screening affects the trend of the astrophysical factor at astrophysical energies. Particle x is virtual so the $A(x,b)B$ astrophysical process is half-off-energy-shell (HOES) and cannot be simply juxtaposed with the corresponding direct one (on-energy-shell, OES) [10]. The modified R-matrix approach has been introduced to extract the astrophysical S-factor of interest from the quasi-free (QF) reaction yield, accounting for HOES effects in the complex multi-resonance scenario.

The use of the THM is particularly suited for the investigation of the ^{27}Al(p,α)^{24}Mg reaction at astrophysical energies. Though this reaction influences several astrophysical scenarios (see [12] and references therein), the widely adopted rate for astrophysical predictions from [13] at $T_9 = 0.1$ shows a lower, median and upper value of 1.85×10^{-11}, 4.34×10^{-11} and 8.51×10^{-11} cm^3 mol^{-1} s^{-1}, respectively, covering almost one order of magnitude, and the uncertainty range becomes larger at lower temperatures. The THM made it possible to reach down to zero energy, casting light on the energy region of astrophysical interest, below about 100 keV. To this purpose, a ^{27}Al projectile was accelerated onto a deuteron target nucleus, having a very simple $p+n$ structure, the $p-n$ motion taking place essentially in s-wave [14]. By selecting small $p-n$ relative momenta, corresponding to large $p-n$ relative distances, ^{27}Al interacts only with the proton which is the participant in the Trojan horse reaction, while the neutron is emitted without taking part in the ^{27}Al+p interaction (therefore it is labelled as spectator). ^{28}Si excited states were populated, later decaying into the ^{24}Mg+α channel to be selected in the offline analysis. Since the beam energy is compensated for by the deuteron binding energy, the ^{27}Al+p reaction can take place in the energy region of astrophysical relevance.

Figure 1 shows the result of the THM measurement. As described in [11, 12], where the whole data analysis is described in detail, the ^{2}H(^{27}Al,α^{24}Mg)n QF cross section is characterized by several resonances, in accordance with what expected from the inspection of the ^{27}Al(p,α)^{24}Mg astrophysical factor. Focusing first on the energy region of

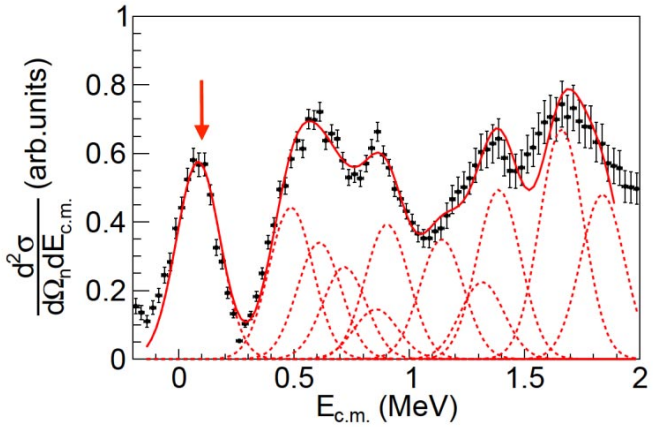

Fig. 1. – Double differential cross section of the ^{2}H(^{27}Al,α^{24}Mg)n reaction (black circles). The red solid line is the result of the fitting using eq.A5 of [15]. Dashed lines mark the contribution of each resonance. The shape of each resonance is determined by convoluting the theoretical shape with the response function taking into account the experimental effects (above all the angular resolution), by means of a devoted Monte Carlo simulation (as described in [12]). A red arrow is used to highlight the energy region of astrophysical interest.

astrophysical interest around 100 keV, we could fit very well the lowest energy peak with a single resonance centered at 84.3 keV. For this resonance we could provide a value of the strength for the first time: $1.67 \pm 0.32 \times 10^{-14}$ eV, while previous works [16] could only set an upper limit $\omega\gamma \leq 2.60 \times 10^{-13}$ eV. The procedure adopted for the extraction of the resonance strengths and their normalizion is described in [11, 12]. For the other resonances below about 300 keV, more stringent upper limits than in [16] were set, while resonance strengths of levels above 300 keV were in good agreement with those in the literature [16], making it possible to carry out a further validity test of the method.

Using the narrow-resonance approximation and the Monte Carlo method that makes use of the code `RatesMC` (see [16] and reference therein), we calculated the reaction rate that turned out to be ~ 3 times lower than in [13] at temperatures where the MgAl cycle is especially important. These results suggest that the MgAl cycle would not be closed at such temperatures (T$\geq$0.055 GK), though further measurements of the ^{27}Al(p,γ)^{28}Si reaction as well would be necessary. Preliminary astrophysical calculations of AGB star nucleosynthesis shows that the new ^{27}Al(p,α)^{24}Mg reaction rate increases the ^{27}Al yields of the stars experiencing soft hot bottom burning up to $\sim 25\%$, for solar metallicity in the $4 - 5$ M$_\odot$ mass domain.

3. – The ANC applied to the ^{3}He$(\alpha,\gamma)^7$Be and ^{6}Li$(p,\gamma)^7$Be reactions

The cross section of a $A(a,\gamma)B$ radiative capture reaction can be expressed at low energies through the matrix element $M = \langle \psi_B \left| O\left(r_{Aa}\right) \right| \psi_A \chi_a \rangle$, where $O\left(r_{Aa}\right)$ is the radial part of the electromagnetic multipole operator depending on the distance r_{Aa} of the projectile and the target nucleus. The wave functions ψ_A and ψ_B correspond to the initial state of the nucleus A and to the final state of the nucleus B following a-capture, while χ_a represents the wave function of the incident particle a (assumed structureless). M is therefore proportional to the $B = A + a$ overlap function; at an asymptotic distance it can be described as the product of the ANC $C_{Aal_Bj_B}$ and the Whittaker function [17].

So, when the reaction is peripheral, namely, when only the outer part of the nuclear radial integrals contributes to the cross section, the cross section of a $A(a,\gamma)B$ radiative capture is proportional to the square of the ANC $C_{Aal_Bj_B}$.

The important point in the application of the ANC method is that such ANCs can be deduced from transfer reactions such as $A(C,D)B$ where $C = D + a$ is used to transfer particle a and populate the B system. To this purpose, the $A(C,D)B$ differential cross sections are fitted using, for instance, the DWBA approach and from the DWBA differential cross section calculated at the main maximum of the angular distribution the relevant ANCs can be deduced as described in [18]. As in the THM case, the deduced cross sections are devoid of electron screening effects and can reach down to zero energy with no need of extrapolation. However, in general only the direct capture contribution to the total radiative capture cross section can be established in the ANC framework. A further advantage of the method is that ANC provides the absolute normalization of direct capture cross sections. In many cases, theoretical calculations can reproduce the trend of the cross sections, so the use of the ANC is especially important, and this is one of the reasons we applied the ANC approach to the investigation of the ^{3}He$(\alpha,\gamma)^7$Be reaction.

3˙1. *The ^{3}He(α,γ)^{7}Be radiative capture reaction.* – The ^{3}He(α,γ)^{7}Be reaction is among the key processes in nuclear astrophysics. It is the first reaction of the 2^{nd} and 3^{rd} $p-p$ chain branch and for such a reason the uncertainty of its rate has a prominent influence on the predicted flux of ^{7}Be and ^{8}B neutrinos. While the detection of the solar neutrinos has become more and more precise after the construction of large neutrino detectors, the ^{3}He(α,γ)^{7}Be reaction remained critical, despite the large number of experimental and theoretical studies devoted to it (see [19] for an extensive discussion). In particular, while the flux of the $p-p$ neutrinos was measured with a precision of 3.4% by the BOREXINO, SNO and Super-Kamiokande collaborations [20-22], present-day uncertainties of affecting the ^{3}He(α,γ)^{7}Be are of the order of 5-8% [23] contrary to the 3% precision required [24, 25].

As discussed in [19,26], by studying the near barrier ^{6}Li(^{3}He,d)^{7}Be α particle transfer reaction, the ANCs for the ^{3}He(α,γ)^{7}Be reaction were obtained. Since the ^{3}He(α,γ)^{7}Be reaction at stellar energies is a pure external direct capture process [27], it proceeds through the tail of the nuclear overlap function, with no sensitivity to nuclear structure details, so our approach made it possible to deduce the $S_{34}(0)$ factor of the ^{3}He(α,γ)^{7}Be reaction with high accuracy.

The transfer reaction was measured using the ^{3}He beams provided by the accelerator of the Department of Physics and Astronomy of the University of Catania (Italy) and the FN tandem accelerator at the John D. Fox Superconducting Accelerator Laboratory at the Florida State University, Tallahassee (FL), USA. To deduce the ANCs, deuteron angular distributions were measured at energies close to the Coulomb barrier over a broad angular range. The ANCs for the $^3\mathrm{He}+\alpha \rightarrow {}^7$Be channel were deduced in the DWBA framework [17] assuming one step proton and α particle transfer. By normalizing the calculated differential cross sections to the experimental ones at backward angles, the ANCs for $^3\mathrm{He}+\alpha \rightarrow {}^7\mathrm{Be}_{\mathrm{g.s}}$ and $^3\mathrm{He}+\alpha \rightarrow {}^7$Be(0.429 MeV) (namely, ^{7}Be first excited state) channels were deduced. The values of the square of the ANCs for the $^3\mathrm{He}+\alpha \rightarrow {}^7$Be(g.s.) and $^3\mathrm{He}+\alpha \rightarrow {}^7$Be(0.429 MeV) are equal to $C^2 = 20.84 \pm 1.12$ [0.82; 0.77] fm^{-1} and $C^2 = 12.86 \pm 0.50$ [0.35; 0.36] fm^{-1}, respectively. The uncertainties include both experimental ones on the $d\sigma^{\mathrm{exp}}/d\Omega$ (first term in square parentheses) and the uncertainty due to the ANC of $d+^4He \rightarrow {}^6$Li, as well as the model uncertainties (second term in square

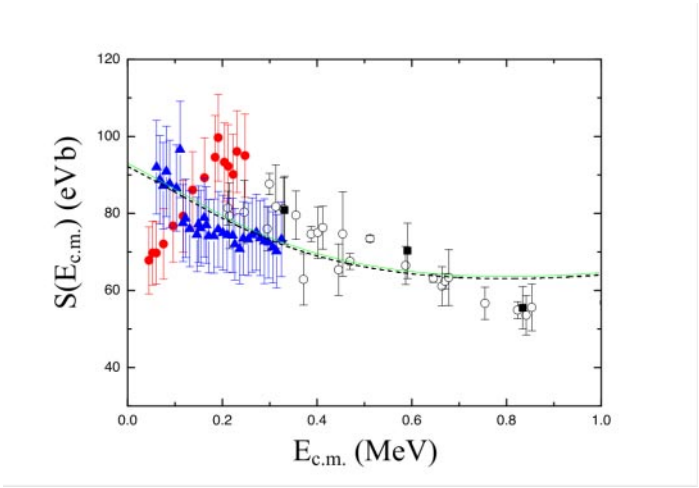

Fig. 2. – The experimental and ANC astrophysical S-factor for the radiative-capture ^{6}Li$(p,\gamma)^7$Be reaction. The solid green line is the calculated direct component of the S-factor, obtained using the ANC values from the near-barrier proton transfer reaction. The black dashed line is the astrophysical factor calculated from the ANCs deduced from [30] experimental data, as a cross check of the method. Blue solid triangles represent the electron-screening corrected S-factor from [30] (including systematic error), red filled circles are the S-factor in [29], empty circles are taken from [31] and black solid squares from [32].

parentheses). Then, the direct capture contribution to the ^{3}He(^{4}He,γ)^{7}Be astrophysical factor was derived within the modified two-body potential model (MTBPM) [19,26], and the resulting $S_{34}(0)$ and $S_{34}(23$ keV) factors (23 keV being the most relevant energy for Solar fusion) were found to be $S_{34}(0) = 0.534 \pm 0.025$ [0.015; 0.019] keVb and $S_{34}(23$ keV$) = 0.525 \pm 0.022$ [0.016; 0.016] keVb. The comparison with the values in the literature shows an improved accuracy with respect to the present-day recommended value in [27] but with an uncertainty still higher than the target value, calling for more work to further reduce it.

3˙2. *The* ^{6}*Li*$(p,\gamma)^7$*Be radiative capture reaction.* – From the same data set, by focusing on the angular distributions at forward angles, it was possible to deduce the cross section of the ^{6}Li$(p,\gamma)^7$Be radiative capture reaction (see [26] for details). ^{6}Li has some impact on the understanding of the primordial lithium problem. In fact, the production mechanism of ^{6}Li and ^{7}Li are very different, so the ^{6}Li/^{7}Li ratio can be used to constrain the lithium production mechanisms. For this purpose, an accurate determination of the ^{6}Li$(p,\gamma)^7$Be astrophysical S-factor is needed. However, available experimental data are contradictory and the electron screening effect has to be taken into account.

After NACRE [28], a new measurement [29] claimed the occurrence of a $J^\pi = (1/2^+, 3/2^+)$ state in ^{7}Be located at about 200 keV above the ^{7}Be$\rightarrow p+^6$Li threshold, not observed in previous works. This discrepancy triggered a new independent experiment [30], covering the same energy region, suggesting a non-resonant low-energy S-factor, thus challenging the occurrence of the 200 keV resonance.

By normalizing the calculated differential cross sections to the measured ones, the ANC values for $^6\mathrm{Li} + p \rightarrow {}^7$Be system, including channels coupling effects, were derived. The squared ANCs (C_p^2) and their uncertainties for $^6\mathrm{Li} + p \rightarrow {}^7$Be turned out to equal $4.51 \pm 0.21\,[0.15;\,0.15]\,\mathrm{fm}^{-1}$ for the ground and $4.37 \pm 0.44\,[0.31;0.31]\,\mathrm{fm}^{-1}$ for the first

excited state of ^{7}Be, respectively. The values in square brackets are the experimental and theoretical uncertainties, respectively. The experimental error is the quadratic sum of the uncertainty of each cross section value, including statistical and normalization errors and the uncertainty of the ANC of the $d + p \rightarrow {}^3$He channel (see [26] for details). The theoretical uncertainty arises from the variation of the geometric parameters of the adopted Woods-Saxon potential, and takes into account non-peripheral effects.

The main contributions to the radiative capture reaction ^{6}Li$(p,\gamma)^7$Be S-factor comes from the $E1$ transition. The contributions of $M1$ and $E2$ are negligible in the astrophysical energy region and were neglected in the calculation. Figure 2 shows the comparison between the the ANC calculated astrophysical factors, starting from the analysis of the ^{6}Li(^{3}He,d)^{7}Be p-transfer reaction (green line) and the experimental data. The indirect $S_{6\,1}(E)$ equals 90.4±2.4 eV·b for E=0 and 89.2±2.3 eV·b for E= 15.1 keV (the Gamow peak energy in the Sun), in excellent agreement with the extrapolated S-factor to zero energy (S(0) = 95 ± 9 eV·b) of [30]. Our results tend to rule out the occurrence of the 200 keV resonance claimed in [29], supporting a smooth increase of the S-factor towards zero energy.

REFERENCES

[1] Iliadis C., *Nuclear Physics of Stars* (Wiley-VCH Verlag GmbH & Co, Weinheim) 2015.
[2] La Cognata M. *et al.*, *Phys. Rev. C*, **72** (2005) 065802.
[3] Tumino A. *et al.*, *Annu. Rev. Nucl. Part. Sci.*, **71** (2021) 345.
[4] Tumino A. *et al.*, *Phys. Lett. B*, **705** (2011) 546.
[5] Cvetinovic A. *et al.*, *Phys. Rev. C*, **97** (2018) 065801.
[6] Rapisarda G. G. *et al.*, *Eur. Phys. J. A*, **54** (2018) 189.
[7] Pizzone R. G. *et al.*, *Eur. Phys. J. A*, **52** (2016) 24.
[8] La Cognata M. *et al.*, *Astrophys. J.*, **805** (2015) 128.
[9] Mukhamedzhanov A. M. *et al.*, *Phys. Rev. C*, **83** (2011) 044604.
[10] Trippella O. *et al.*, *Astrophys. J.*, **837** (2017) 41.
[11] La Cognata M. *et al.*, *Phys. Lett. B*, **826** (2022) 136917.
[12] La Cognata M. *et al.*, *Astrophys. J.*, **941** (2022) 96.
[13] Iliadis C *et al.*, *Nucl. Phys. A*, **841** (2010) 31.
[14] Lamia L. *et al.*, *Phys. Rev. C*, **85** (2012) 025805.
[15] La Cognata M. *et al.*, *Astrophys. J.*, **708** (2010) 796.
[16] Iliadis C *et al.*, *Nucl. Phys. A*, **841** (2010) 251.
[17] Mukhamedzhanov A. M. *et al.*, *Phys. Rev. C*, **56** (1997) 1302.
[18] Burjan V. *et al.*, *Eur. Phys. J. A*, **55** (2019) 114.
[19] Kiss G. G. *et al.*, *Phys. Lett. B*, **807** (2020) 135606.
[20] The Borexino Collaboration, *Nature*, **562** (2018) 505.
[21] Aharmim B. *et al.*, *Phys. Rev. C*, **81** (2010) 055504.
[22] Abe K. *et al.*, *Phys. Rev. C*, **83** (2011) 052010.
[23] Vinyoles N. *et al.*, *Astrophys. J.*, **852** (2017) 202.
[24] Haxton W. C. and Serenelli A. M., *Astrophys. J.*, **687** (2008) 678.
[25] Bahcall J. N. and Pinsonneault M. H., *Phys. Rev. Lett.*, **92** (2004) 121301.
[26] Kiss G. G. *et al.*, *Phys. Rev. C*, **104** (2021) 015807.
[27] Adelberger E. G. *et al.*, *Rev. Mod. Phys.*, **83** (2011) 195.
[28] Angulo C. *et al.*, *Nucl. Phys. A*, **656** (1999) 3.
[29] He J. J. *et al.*, *Phys. Lett. B*, **725** (2013) 287.
[30] Piatti D. *et al.*, *Phys. Rev. C*, **102** (2020) 052802.
[31] Switkowski Z. E. *et al.*, *Nucl. Phys. A*, **50** (1979) 331.
[32] Amar A. and Burtebayev N., *J. Nucl. Sci.*, **1** (2014) 15.